PERGAMON

International Journal of Heat and Mass Transfer 45 (2002) 2611–2622

International Journal of HEAT and MASS TRANSFER

www.elsevier.com/locate/ijhmt

Dynamics of three-dimensional temperature field in electrical system of floor heating

Jerzy Gołębiowski, Sławomir Kwieĉkowski *

Technical University of Białystok, Grunwaldzka St. 11/15, 15-893 Białystok, Poland

Received 1 September 2000; received in revised form 1 April 2001

Abstract

In the paper dynamics of a three-dimensional temperature field in the system of direct floor heater was investigated. A step response (heating on curve) and local and global time constants of the device were determined. Then, a spatial–temporal distribution of the field in the system controlled by the on–off regulator was found. The mathematical model of heat propagation was a non-homogeneous and homogeneous equation of a three-dimensional diffusion with an adequate set of boundary conditions. Four methods were applied for the solution of the above: superposition of states (coupled with separation of variables), finite elements, criterion of an averaged time constant and superposition of step characteristics. It was found that time profiles of the temperature depend very strongly on the position of an observing point. All relations were processed numerically. The obtained results are presented in a graphic form. A physical interpretation of the achieved solutions is included. © 2002 Elsevier Science Ltd. All rights reserved.

Keywords: Transient thermal field; Electrical floor heating; Parabolic boundary problem

1. Introduction

The paper is a continuation of the recent publications of the authors [1–3]. In [1,2] a stationary component of the temperature field in a direct floor heater was determined. In [3] dynamics of the two-dimensional temperature field in a long heating duct was investigated. The considerations given in [3] were referred to the heaters, whose length is considerably larger than the cross-sectional dimensions (i.e. in hallways, horticultural tunnels, communication ducts, etc.). The above assumption is not fulfilled in the compartments of a small and medium size. Therefore it is necessary to extend the results of the paper [3] to a three-dimensional case.

The system will be considered, whose simplified scheme is presented in Fig. 1. As it is seen, the axes of cable sections are passing through the points of co-ordinates (x_k, y_k, z), where $x_k = 2a(k-0.5)/K$, $y_k = y_1 =$ const., $z \in \langle ul, (1-u)l \rangle$. More accurate description of the heater and the assumed simplifications are given in [2].

The aim of the present paper is the investigation of dynamic properties of a three-dimensional system and the analysis of transient (i.e. time-spatial) temperature field distributions.

2. Step response of the system (heat-up curve)

For the following reasons the step response has a special place [4,7] in the analysis of system dynamics:

(a) it is a convenient connection between the investigations of steady and transient states (e.g. between [1,2] and [3] and the present paper),
(b) it enables direct (e.g. Section 3.4) or indirect (e.g. by means of Duhammel's theorem [14]) determination of the response on an arbitrary excitation,
(c) it is a basis for determination of the averaging time constant [5,6] of the objects with distributed parameters and their transmittances.

In the analysed case the step characteristic is the system thermal response $H(x, y, z, t)$ for the switching on of the

* Corresponding author. Tel.: +48-85-742-1657; fax: +48-85-742-1657.

E-mail address: kwiecie@cksr.ac.bialystok.pl (S. Kwieĉkowski).

0017-9310/02/$ - see front matter © 2002 Elsevier Science Ltd. All rights reserved.
PII: S0017-9310(01)00353-2

Nomenclature

A	dimensionless constant, determined by (4c)
$(2a, 2b, l)$	dimensions of a floor panel (Fig. 1)
$(2a^*, 2b, l)$	dimensions of repeatable segment (Fig. 2)
$[C]$	heat capacity matrix
c	specific heat of concrete
$G(\cdots)$	transmittance of the first-order element
$g(x, y, z, t)$	volumetric power density of spatial heat sources (at a stationary case $g(x, y, z)$)
$\{g\}$	vector of heat sources
$H(x, y, z, t)$	temperature step response of the system (heating on curve)
$H_t(x, y, z, t)$	transient component of a temperature step response of the system
$H_s(x, y, z)$	steady component of the temperature step response of the system
$\{\dot{H}\}$	vector of the step response derivative at nodes
K	number of cable sections
k	index of the kth cable section ($k = 1, 2, 3, \ldots, K$)
q_k	linear power density of the kth cable sector
R	cable radius
r	radius of the cable resistive core
s	Laplace's transformation variable,
$T(x, y, z, t)$	entire temperature field in the floor panel
$T_1(x, y, z, t')$	temperature field of the floor panel at the second stage of operation of the regulated system (first self-cooling)
$T_2(x, y, z, t'')$	temperature field of the floor panel at the third stage of operation of the regulated system (repeated heating on)
$T_{2t}(x, y, z, t'')$	transient component of the temperature at the third stage of operation of the regulated system (repeated heating on)
T_H	the temperature of power switching off
T_L	the temperature of power switching on
T_0	ambient temperature
$\{T\}$	nodal temperature vector
t	time
t', t''	changed time axes at the second ($'$) or third ($''$) stage of operation of the regulated system
t_1	the time of first heating of the floor (start-up)
t_2	the time of first self-cooling of the floor
t_3	the time of second heating of the floor
u	dimensionless coefficient of filling of the length l by the cable (Fig. 1(b), $u \in \langle 0, 1 \rangle$)
(x, y, z)	coordinates of a point in the floor panel
(x^*, y^*, z^*)	coordinates of the regulator sensor location within the floor panel
(x_k, y_k, z)	coordinates of the position of the kth section of the cable core
y_1	plane of the cable layout
α	averaging coefficient of heat transfer to air (sum of the radiation and convection coefficients)
γ_n	consecutive positive roots of the transcendental Eq. (4c)
δ	density of concrete
$\delta_{m0}, \delta_{(2i)0}$	Kronecker's symbols
ε	index of the series convergence
λ	average heat conductivity of concrete
$[\lambda]$	generalised heat conductance matrix
$v_1(x, y, z, t')$	increase (15) of the temperature at the second stage of operation of the regulated system
$v_{mni}^{(k)}(x, y, z)$	series term (4a)
$\tau(x, y, z)$	local time constant
τ_g	global time constant
χ	diffusivity ($= \lambda/(c\delta)$)
$\mathbf{1}(\cdots)$	unit step function

power supply at the zero time instant ($t = 0$). For $t > 0$ the process of a heat diffusion modelled by a non-homogeneous parabolic equation [8,9,14] will proceed

$$\frac{\partial^2 H(x,y,z,t)}{\partial x^2} + \frac{\partial^2 H(x,y,z,t)}{\partial y^2} + \frac{\partial^2 H(x,y,z,t)}{\partial z^2} - \frac{1}{\chi}\frac{\partial H(x,y,z,t)}{\partial t} = -\frac{1}{\lambda} g(x,y,z) \tag{1}$$

for $0 \leqslant x \leqslant 2a$, $0 \leqslant y \leqslant 2b$, $0 \leqslant z \leqslant l$.

Boundary conditions of the system were precisely described in [1,2]. It was assumed that the heater does not exchange energy through the thermally insulated walls

$$\left.\frac{\partial H(x,y,z,t)}{\partial x}\right|_{x=0} = 0, \tag{2a}$$

$$\left.\frac{\partial H(x,y,z,t)}{\partial x}\right|_{x=2a} = 0, \tag{2b}$$

$$\left.\frac{\partial H(x,y,z,t)}{\partial y}\right|_{y=0} = 0, \tag{2c}$$

$$\left.\frac{\partial H(x,y,z,t)}{\partial z}\right|_{z=0} = 0, \tag{2d}$$

$$\left.\frac{\partial H(x,y,z,t)}{\partial z}\right|_{z=l} = 0, \tag{2e}$$

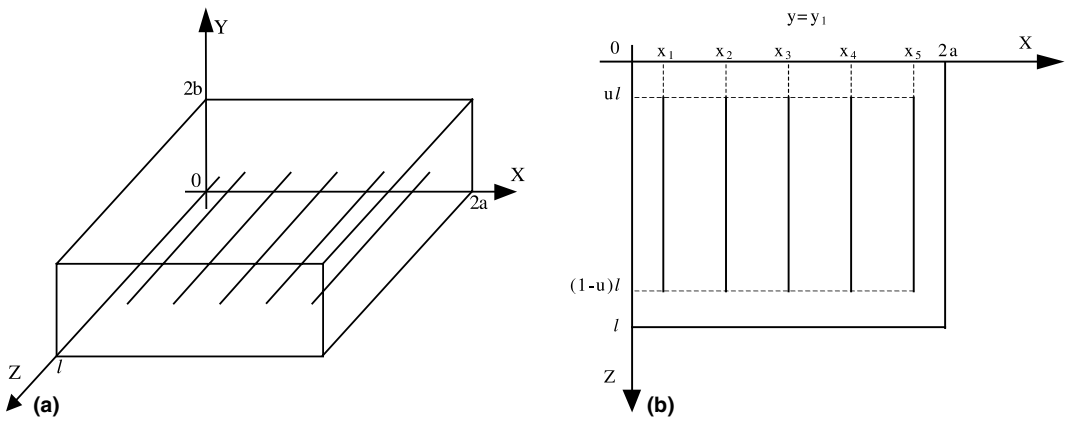

Fig. 1. Electric floor heater: (a) simplified scheme; (b) cross-section at height of the cable.

and that the heat is emitting throughout the upper surface $y = 2b$ in accordance with Newton's law

$$\left.\frac{\partial H(x,y,z,t)}{\partial y}\right|_{y=2b} = -\frac{\alpha}{\lambda}[H(x,y=2b,z,t) - T_0]. \tag{2f}$$

At the moment $t = 0$ the system remains in a steady state and all its points have the temperature T_0:

$$H(x,y,z,t=0) = T_0. \tag{2g}$$

In the present paper, the step characteristic was determined by means of three methods: (a) superposition of states, (b) averaging time constant, (c) finite element method. After a presentation of the consecutive solutions, computational examples will be presented in the continuation of the section.

2.1. Method of the states superposition

In the method of the states superposition the solution of the boundary problem (1), (2a)–(2g) is anticipated in the form

$$H(x,y,z,t) = H_s(x,y,z) + H_t(x,y,z,t), \tag{3}$$

where

$$\lim_{t\to\infty} H(x,y,z,t) = H_s(x,y,z), \quad \lim_{t\to\infty} H_t(x,y,z,t) = 0.$$

If the cable will be substituted by the sections of its axis with the length of $l(1-2u)$ each, then the steady component is expressed as below [2, formulas (8) and (11)]

$$H_s(x,y,z) = T_0 + \sum_{k=1}^{K}\sum_{m=0}^{\infty}\sum_{n=1}^{\infty}\sum_{i=0}^{\infty} v_{mni}^{(k)}(x,y,z), \tag{4a}$$

where

$$v_{mni}^{(k)}(x,y,z) = \frac{2q_k}{ab\pi\lambda}\frac{(-1)^i\cos\left(m\pi\frac{x_k}{2a}\right)\cos\left(\gamma_n\frac{y_k}{2b}\right)\sin[i\pi(1-2u)]}{i(1+\delta_{m0})(1+\delta_{(2i)0})\left[1+\frac{\sin(2\gamma_n)}{2\gamma_n}\right]} \times \frac{\cos\left(m\pi\frac{x}{2a}\right)\cos\left(\gamma_n\frac{y}{2b}\right)\cos\left(2i\pi\frac{z}{l}\right)}{\left[\left(\frac{m\pi}{2a}\right)^2+\left(\frac{\gamma_n}{2b}\right)^2+\left(\frac{2i\pi}{l}\right)^2\right]}, \tag{4b}$$

$$\operatorname{ctg}\gamma_n = \frac{\gamma_n}{A}, \quad A = \frac{2\alpha b}{\lambda}. \tag{4c}$$

From formulas (4a)–(4c) it follows that in the present section it is enough to determine a transient component only. Taking advantage of (1), (2a)–(2g) and (3), the boundary problem with respect to $H_t(x,y,z,t)$ was formulated:

$$\frac{\partial^2 H_t(x,y,z,t)}{\partial x^2} + \frac{\partial^2 H_t(x,y,z,t)}{\partial y^2} + \frac{\partial^2 H_t(x,y,z,t)}{\partial z^2} - \frac{1}{\chi}\frac{\partial H_t(x,y,z,t)}{\partial t} = 0 \tag{5}$$

for $0 \leqslant x \leqslant 2a$, $0 \leqslant y \leqslant 2b$, $0 \leqslant z \leqslant l$, $t > 0$,

$$\left.\frac{\partial H_t(x,y,z,t)}{\partial x}\right|_{x=0} = 0, \tag{6a}$$

$$\left.\frac{\partial H_t(x,y,z,t)}{\partial x}\right|_{x=2a} = 0, \tag{6b}$$

$$\left.\frac{\partial H_t(x,y,z,t)}{\partial y}\right|_{y=0} = 0, \tag{6c}$$

$$\left.\frac{\partial H_t(x,y,z,t)}{\partial z}\right|_{z=0} = 0, \tag{6d}$$

$$\left.\frac{\partial H_t(x,y,z,t)}{\partial z}\right|_{z=l} = 0, \tag{6e}$$

$$\left.\frac{\partial H_t(x,y,z,t)}{\partial y}\right|_{y=2b} = -\frac{\alpha}{\lambda}H_t(x,y=2b,z,t), \tag{6f}$$

$$H_t(x,y,z,t=0) = -\sum_{k=1}^{K}\sum_{m=0}^{\infty}\sum_{n=1}^{\infty}\sum_{i=0}^{\infty} v_{mni}^{(k)}(x,y,z). \tag{6g}$$

The variables in Eq. (5) were separated [8]. The eigenfunctions are sinuses and cosinuses (with respect to spatial variables) and an exponential function (with respect to time). The sinuses were discarded on the basis of (6a), (6c) and (6d). The problem eigenvalues were

determined from the boundary conditions (6b), (6e) and (6f). Consequently, the coefficient of appropriate series follows from the initial condition (6g). This way the solution $H_t(x,y,z,t)$ was obtained. The investigated step characteristic (heat-up curve) was determined connecting $H_t(x,y,z,t)$ with formulas (3) and (4a)–(4c):

$$H(x,y,z,t) = T_0 + \sum_{k=1}^{K}\sum_{m=0}^{\infty}\sum_{n=1}^{\infty}\sum_{i=0}^{\infty} v_{mni}^{(k)}(x,y,z) \times \left[1 - \exp\left(-\frac{t}{\tau_{mni}}\right)\right], \tag{7a}$$

where

$$\tau_{mni} = \left\{\left[\left(\frac{m\pi}{2a}\right)^2 + \left(\frac{\gamma_n}{2b}\right)^2 + \left(\frac{2i\pi}{l}\right)^2\right]\chi\right\}^{-1}, \tag{7b}$$

$v_{mni}^{(k)}(x,y,z)$ is given in (4b).

In the above analytical model the heat sources were assumed to be linear (W/m) [2, Sections 2.1 and 3.1]. For this reason, the field source points are singular (at the coordinates $x_k,\ y_k = y_1,\ z \in \langle ul, (1-u)l\rangle$). Hence tabulating (7a) requires an introduction of some deviation of the abscissa $x = x_k$. It was assumed that in the nearest surroundings of a source, the deviation is equal to the cable radius R [2, Fig. 2]. In the rest of the area the deviation can be less and it is equal to the radius r of the cable resistive core (usually $r = R/6$). Besides, a convergence control of (7a) is necessary by the use of an index ε. Namely, the summation of (7a) can be interrupted, when the quotient of the modulus of the sum of the last 10 terms by the modulus of the total sum is less than ε. The above remarks have an important significance for the numerical tabulation of the characteristic (7a).

2.2. Approximation of the dynamics by the first-order element

Characteristic (7a) is a quadruple sum (infinite with respect to indices m,n,i and finite with respect to k). An estimation of the transient duration by the use of (7a) is therefore very difficult. Such an estimation is enabled by the well-known criterion of the averaging time constant (cf. [5, Section 3] and [6, formula (11)]):

$$\tau(x,y,z) = \int_0^{\infty} \frac{H(x,y,z,t) - H_s(x,y,z)}{H(x,y,z,t=0) - H_s(x,y,z)}\,\mathrm{d}t. \tag{8a}$$

Introducing (2g), (4a) and (7a) into (8a) a local time constant was obtained (i.e. at the point (x,y,z))

$$\tau(x,y,z) = \frac{\sum_{k=1}^{K}\sum_{m=0}^{\infty}\sum_{n=1}^{\infty}\sum_{i=0}^{\infty} v_{mni}^{(k)}(x,y,z)\tau_{mni}}{\sum_{k=1}^{K}\sum_{m=0}^{\infty}\sum_{n=1}^{\infty}\sum_{i=0}^{\infty} v_{mni}^{(k)}(x,y,z)}. \tag{8b}$$

Relation (8b) is easy for the computerised tabulation (after utilising formulas (4b) and (7b)). The averaging time constant of the whole system (i.e. global) was determined averaging the local constant at N points

$$\tau_g = \frac{1}{N}\sum_{r=1}^{N}\tau(x_r,y_r,z_r). \tag{8c}$$

The time of the thermal disturbance persistence can be estimated as equal to $4\tau_g$. The introduction of $\tau(x,y,z)$ also simplifies formula (7a) (the expression in square brackets can be shifted before the symbol of a sum)

$$H(x,y,z,t) = T_0 + \left\{1 - \exp\left[-\frac{t}{\tau(x,y,z)}\right]\right\} \times \sum_{k=1}^{K}\sum_{m=0}^{\infty}\sum_{n=1}^{\infty}\sum_{i=0}^{\infty} v_{mni}^{(k)}(x,y,z). \tag{9a}$$

Replacing $\tau(x,y,z)$ in the above relation by τ_g:

$$\tau(x,y,z) \to \tau_g, \tag{9b}$$

a less accurate approximation of the characteristic (7a) was obtained. From formulas (9a) and (9b) it follows that the system dynamics at the given point of the region was approximated by the first-order element. Its transmittances are

$$G(x,y,z,s) = \frac{1}{1+s\tau(x,y,z)} \quad \text{or} \quad G(s) = \frac{1}{1+s\tau_g}.$$

2.3. Finite element method

The boundary problem (1), (2a)–(2g) was solved among other things by means of the finite element method [10,11] using the professional program NISA II/Heat Transfer of the American firm EMRC [12]. The heat sources were approximated by regular octagonal prisms [2, Fig. 3(b)] inscribed into the cable core cylinder of the radius r [2, Fig. 2(b)]. The mentioned prisms were formed from even-armed wedge elements, whose vertexes are located on the cable axis. In these conditions the function which appeared on the right-hand side of (1) will take the following form:

$$g(x,y,z) = \begin{cases} g_0 = \text{const.} & \text{at interior octagonal prisms [2, Fig. 3(b)],} \\ 0 & \text{at the rest of area.} \end{cases} \tag{10}$$

The power of such a virtual source has to be the same as the power of the real cable and its stationary analytical model [2]. On this basis the volumetric heat efficiency g_0 is determined in formula (10). The rest of a source-free region was partitioned on quadrangular prisms. This way a mesh was developed, whose fragment is shown in [2, Fig. 3(a)]. After finding the proper figure in [2] it is seen that the mesh was refined at the surroundings of field sources (for the sake of the large temperature gradient in the cable surroundings).

In the program NISA II the Galerkin procedure was applied [12,13]. It discretises problem (1), (2a)–(2e), (2g) with respect to the spatial variables. In the consequence, problem (1), (2a)–(2g) was reduced to the system of the first-order differential equations with respect to time:

$$[C]\{\dot{H}\} + [\lambda]\{H\} = \{g\}. \tag{11}$$

It should be pointed out that $[\lambda]$ and $\{g\}$ contain the components derived from the convectional boundary condition (2f).

In the program NISA II four methods of a differential discretisation of system (11) with respect to time are accessible [12]. Because of the solution stability and weak limitation of the time step the method of backward difference quotient was chosen [11]. In the consequence of that (at each time step) the system of algebraic equations was obtained with respect to the temperature at all nodes. For a solution of the mentioned system the Newton–Raphson method was used [18]. This way the investigated vector $\{H\}$ was determined, which accomplished the procedure.

2.4. Examples of the heat-up curve computations and discussion of the results

Relations (7a), (7b) and (9a), (9b) and vector $\{H\}$ (Section 2.3) are the searched step responses (heat-up curves) of the system investigated. Because the cable is laid symmetrically, the characteristics can be presented in the so-called repeatable segment [2, Chapter 4.1]. It is a constrained computational area shown in Fig. 2. Hence in all the relations $K = 1$ and $a = a^*$ should be introduced.

The following set of data was assumed:

$\lambda = 1$ W/(m K), $c = 840$ J/(kg K),

$\delta = 2000$ kg/m^3, $\alpha = 12$ W/(m^2 K),

$q_k = 15$ W/m, $g_0 = 2.1213 \times 10^7$ W/m^3,

$T_0 = 20$°C, $2a^* = 0.12$ m,

$2b = 0.06$ m, $x_k = x_1 = 0.06$ m,

$y_k = y_1 = 0.015$ m, $l = 2.5$ m,

$u = 0.1$, $r = 5 \times 10^{-4}$ m,

$R = 3 \times 10^{-3}$ m, $\varepsilon = 10^{-7}$.

Computations were performed on the computer Pentium II 233 MHz. The repeatable segment was partitioned on 6000 finite elements with a total number of 7171 nodes [2, Fig. 3(a)].

A convergence of the series (7a), (7b) and (9a), (9b) was controlled by the method given above (the end of Section 2.1). The summation of the series (7a), (7b) required the largest number of terms at the point of the least deviation from the singular plane ($x = 0.06 \pm 5\times 10^{-4}$ m, $y = 0.06$ m, $z = 0.25$ m). The following information refers to that extreme location. The steady and transient components of the distribution (7a), (7b) were computed separately.

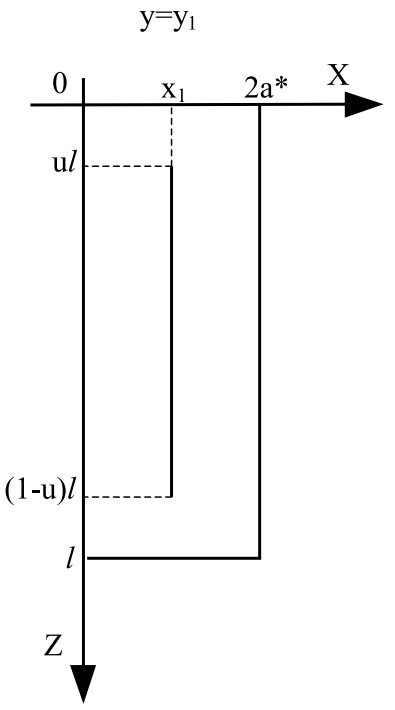

Fig. 2. Repeatable segment of the heater (cross-section at height of the heating cable).

The steady component is described by the expression (4a) contained in (7a) and (9a) and at the denominator of (8b). In (4a)–(4c), an indeterminate term for $i = 0$ was separated, whose value was determined by means of the asymptotic limit $i \to 0$. After subsequent transformations of (4a)–(4c) the series with index m were summated analytically according to [1, formula (9)]. In this manner the relations [2, formulas (10)] were obtained in which one less series appeared. It limited the maximal number of terms in [2, formula (10b)] up to 322 and up to 322×5022 in [2, formula (10c)].

In the transient component of (7a) the exponential function appeared. So the relation [1, formula (9)] has not found an application. For this reason the transient component remained as the triple series ($K = 1$). It is slowly convergent for the small values of time (for $t = 0$ $309 \times 1564 \times 4756$ terms were summated). The convergence increases with time (e.g. for $t = 10\,800$ s the number of considered terms was reduced to $11 \times 11 \times 11$, which is a minimum following from the assumed convergence criterion).

The maximal number of terms in the numerator of relation (8b) did not exceed $33 \times 604 \times 4486$. This is a relatively good convergence following from formula

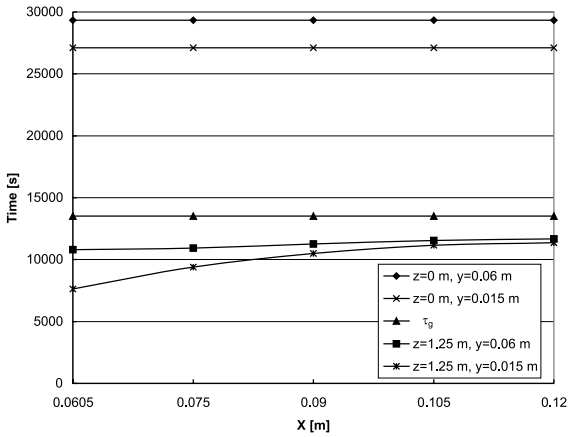

Fig. 3. Distribution of the local time constant in the selected cross-sections and global time constant ($\tau_g = 13502.86$ s).

(7b). The global time constant (8c) was determined averaging 99 local constants.

The results of computations are presented in Figs. 3–5. Fig. 3 illustrates the local time constant distribution. Because $4\tau(x, y = 0.015 \text{ m}, z) < 4\tau(x, y = 0.06 \text{ m}, z)$, the time of the transient persistence is shorter in the cable horizontal plane than on the floor surface. The temperature increases more slowly in the peripheral region comparing to the central zone with the cable $(4\tau(x, y, z = 1.25 \text{ m}) < 4\tau(x, y, z = 0 \text{ m}))$, because the heat diffusion is faster in the surroundings of energy sources than at more distant points. This fact is also illustrated in Figs. 4 and 5 by the lines without additional marks, obtained by means of the models with distributed parameters (analytical and numerical version). A fast increase of temperature on the cable surface is observed in Fig. 5(a), whereas a delay of the characteristic is evident in Figs. 4 and 5(b) (it concerns the start of the transient). Therefore the presented results have a good physical interpretation.

Comparing the methods of the step characteristic determination the following remarks resulted:

(a) Approximation by the global time constant is the least accurate (Figs. 4 and 5). It is clearly evident in the cable surroundings (Fig. 5(a)), where an initial speed of the heat penetration is significantly greater.
(b) Approximation by the local time constant is the least accurate at the beginning of the transient (Figs. 4 and 5(a)). The first-order element cannot precisely model typical field effects (apparent dead time or intensive diffusion). The smallest error of an approximation by the local time constant occurred in the middle part of the segment surface (Fig. 5(b)).
(c) The difference between the numerical and analytical solution is the largest in the direct surroundings of the cable (Fig. 5(a)). It follows from the assumed different models of the cable core: linear (Section 2.1) and volumetric (Section 2.3) heat source.

From Fig. 5(b) it follows that during the steady state the temperature of the floor surface in the region over the heat source will exceed 30 °C. On the other hand it is known that heating comfort is perceptible at the temperature around 26 °C (Polish standards PN-85/N-08013). Therefore the step response cannot be a normal procedure of work of the floor. It serves only for a determination of the system dynamic properties. By this reason the system controlled by a regulator will be analysed in the following section of the paper.

3. Operation with a regulator

From the preceding section it follows that the heating comfort of a compartment can be ensured by appropriate regulation of the heater. In the complex systems

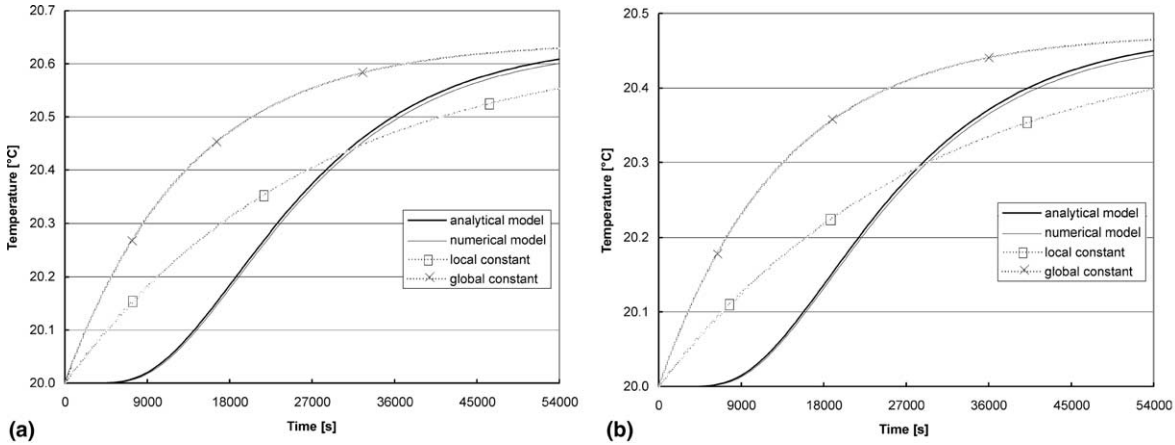

Fig. 4. Step response of the system (heat-up curve) for $x = 0.12$ m, $z = 0$ m: (a) at height of the heating cable $y = 0.015$ m; (b) on the floor surface $y = 0.06$ m.

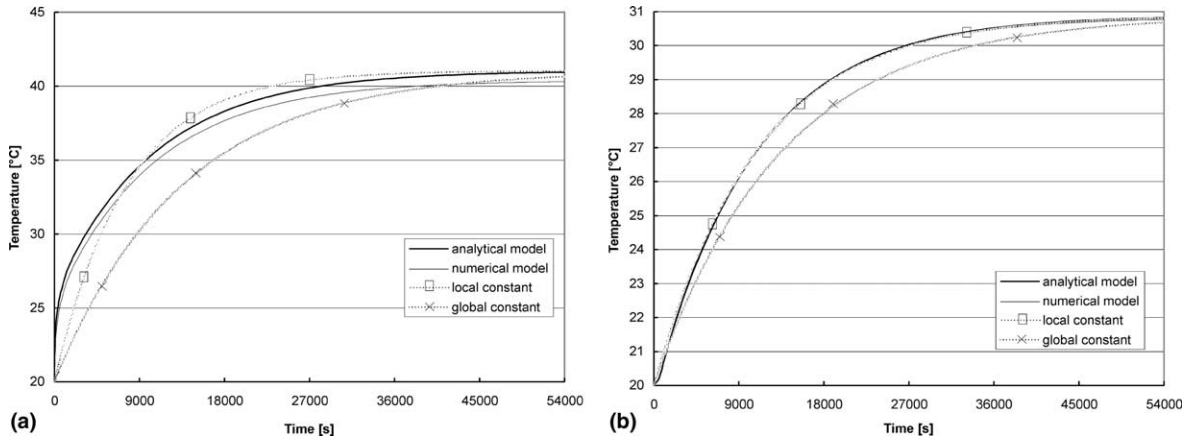

Fig. 5. Step response of the system (heat-up curve) for $x = 0.06$ m, $z = 1.25$ m: (a) at height of the heating cable $y = 0.015$ m; (b) on the floor surface $y = 0.06$ m.

of automatic control there are considered [15,16]: (a) temperature of the floor surface, (b) temperature of air inside and outdoors, (c) individual program of user's needs. In the present paper only the first factor listed above was considered for the regulation [15]. It was assumed that the temperature measuring sensor is installed at the point of co-ordinates (x^*, y^*, z^*). By means of the on–off regulator the temperature of this point is stabilised around a set value. When it exceeds a half of the regulator hysteresis the heater will be switched off. But if the temperature at (x^*, y^*, z^*) declines by half of the hysteresis below the set value, the power supply will be reconnected. The aim of the present section is then determination of the transient temperature field of a three-dimensional system with alternative switching on and off of the device.

The operation of a direct heater is controlled in the above manner [15]. It should be pointed out that in this case moments of the heater switching on and off are not known in advance (except first switching at $t = 0$). It is important difference comparing with the supply manner of an accumulative heater [17]. In [17] the time of the system operation was given in advance. It followed from lower rates of the electric energy at strictly determined intervals of a 24 h period (from the so-called night tariff). Besides, a two-dimensional system was investigated in [17] by means of elementary balances. In the present section four other methods of the field analysis in a three-dimensional system were used.

3.1. Analytical method

Before the first switching off of the power supply at the moment $t = t_1$ (i.e. during start-up of heating) the temperature distribution $T(x, y, z, t)$ is a step characteristic

$$T(x, y, z, t) = H(x, y, z, t) \quad \text{for } 0 \leqslant t \leqslant t_1, \tag{12}$$

where $H(x, y, z, t)$ is determined by formula (7a). The moment t_1 is determined from the condition

$$T(x = x^*, y = y^*, z = z^*, t = t_1) = H(x^*, y^*, z^*, t_1) = T_H. \tag{13}$$

Because function (12) is monotonic with respect to t, then in order to determine t_1 a time step in the surroundings of T_H should be reduced during the tabulation of (12).

At the moment $t = t_1$ a new time axis $t' = 0$ was introduced. For $0 \leqslant t' \leqslant t_2$ the heat sources do not operate and the equation of a conductivity becomes homogeneous (5). Instead of considering the referred for this case distribution $T_1(x, y, z, t')$ with the initial condition

$$T_1(x, y, z, t' = 0) = H(x, y, z, t = t_1), \tag{14}$$

it is more convenient to introduce an increase

$$v_1(x, y, z, t') = T_1(x, y, z, t') - T_0. \tag{15}$$

Then it is sufficient to exchange relations (5), (6a)–(6f)

$$H_1(x, y, z, t) \to v_1(x, y, z, t'), \tag{16a}$$

$$t \to t', \tag{16b}$$

where "$a \to b$" denotes "to change a by b". On the basis of (15), (14) and (7a) the boundary problem (16a), (16b) was supplemented with an initial condition

$$v_1(x, y, z, t' = 0) = \sum_{k=1}^{K} \sum_{m=0}^{\infty} \sum_{n=1}^{\infty} \sum_{i=0}^{\infty} v_{mni}^{(k)}(x, y, z) \times \left[1 - \exp\left(-\frac{t_1}{\tau_{mni}}\right)\right], \tag{16c}$$

where $v_{mni}^{(k)}(x, y, z)$ and τ_{mni} determine relations (4b), (7b), respectively. The method of the solution of the

boundary-initial problem (16a)–(16c) was outlined directly after formula (6g). The increase obtained from that was substituted into (15), and afterwards the old time axis $t' = t - t_1$ was restored. It leads to the required temperature distribution at the second stage of the system operation for $t_1 \leqslant t \leqslant t_1 + t_2$:

$$T(x,y,z,t) = T_1(x,y,z,t-t_1) = T_0 + \sum_{k=1}^{K}\sum_{m=0}^{\infty}\sum_{n=1}^{\infty}\sum_{i=0}^{\infty} v_{mni}^{(k)}(x,y,z) \times \left[\left(1-\exp\left(-\frac{t_1}{\tau_{mni}}\right)\right)\exp\left(-\frac{t-t_1}{\tau_{mni}}\right)\right]. \tag{17}$$

The moment t_2 was determined from the condition

$$T(x=x^*, y=y^*, z=z^*, t=t_1+t_2) = T_1(x^*,y^*,z^*,t_2) = T_L, \tag{18}$$

where the monotony of $T_1(x,y,z,t')$ with respect to t' was utilised.

The regulator switches on the power supply again at the moment $t = t_1 + t_2$. A next time axis was then introduced ($t'' = 0$). For $0 \leqslant t'' \leqslant t_3$ the following substitutions were done in (1) and (2a)–(2f):

$$H(x,y,z,t) \to T_2(x,y,z,t''), \tag{19a}$$

$$t \to t''. \tag{19b}$$

This time the initial condition is non-homogeneous

$$T_2(x,y,z,t''=0) = T_1(x,y,z,t'=t_2), \tag{19c}$$

where $T_1(x,y,z,t'=t-t_1)$ follows from (17). The boundary-initial problem (19a)–(19c) was solved by means of the method of the states superposition (Section 2.1). The steady-state component $T_{2s}(x,y,z)$ was determined from (4a):

$$T_{2s}(x,y,z) = H_s(x,y,z). \tag{20}$$

A differential equation and boundary conditions for the transient component $T_{2t}(x,y,z,t'')$ were obtained after introducing the following exchange in (5) and (6a)–(6f):

$$H_t(x,y,z,t) \to T_{2t}(x,y,z,t''), \tag{21a}$$

$$t \to t''. \tag{21b}$$

The initial value of the transient component was determined on the basis of (19c), (17) and (20):

$$T_{2t}(x,y,z,t''=0) = T_2(x,y,z,t''=0) - T_{2s}(x,y,z) = \sum_{k=1}^{K}\sum_{m=0}^{\infty}\sum_{n=1}^{\infty}\sum_{i=0}^{\infty} v_{mni}^{(k)}(x,y,z) \left[\left(1-\exp\left(-\frac{t_1}{\tau_{mni}}\right)\right) \times\exp\left(-\frac{t_2}{\tau_{mni}}\right) - 1\right]. \tag{21c}$$

Solving problem (21a)–(21c) by the known method, superpositioning the result from (20) and returning to the old time axis $t'' = t - t_1 - t_2$ it was finally obtained for $t_1 + t_2 \leqslant t \leqslant t_1 + t_2 + t_3$:

$$T(x,y,z,t) = T_2(x,y,z,t-t_1-t_2) = T_0 + \sum_{k=1}^{K}\sum_{m=0}^{\infty}\sum_{n=1}^{\infty}\sum_{i=0}^{\infty} v_{mni}^{(k)}(x,y,z) \times \left\{\left[\left(1-\exp\left(-\frac{t_1}{\tau_{mni}}\right)\right)\exp\left(-\frac{t_2}{\tau_{mni}}\right) - 1\right] \times \exp\left(-\frac{t-t_1-t_2}{\tau_{mni}}\right) + 1\right\} \tag{22}$$

The moment t_3 was determined analogously to (13), (18):

$$T(x=x^*, y=y^*, z=z^*, t=t_1+t_2+t_3) = T_2(x^*,y^*,z^*,t_3) = T_H. \tag{23}$$

It follows from (13) and (23) that after the moment $t_2 + t_3$ the temperature of the sensor will return to the value of T_H. Hence the time-spatial distributions of the temperature were determined for a full cycle of the system power supply. The remarks with respect to the source points singularity given after formula (7b) were considered during numerical tabulation of relations (12), (17) and (22).

3.2. Numerical method

In the present section the time axis remains unchanged. Consequently, consecutive switching on and off of the power supply should be modelled by a heat source of the efficiency depending on time. For this reason in formulas (1) and (2a)–(2g) it was changed

$$H(x,y,z,t) \to T(x,y,z,t), \tag{24}$$

$$g(x,y,z) \to g(x,y,z,t). \tag{25}$$

The program NISA II/Heat Transfer (the same as for the step characteristic) was applied for solving (24) and (25). The system partition on finite elements, the method of discretisation and solution of (24) and (25) were given in Section 2.3. Moreover, the program contains a standard heat source function [12]. It enables a piecewise linear approximation of the time profile of the power efficiency. In the analysed case, rectangular signals represent the efficiency change (on–off type). But two different values of the power cannot be chosen for the same moment t. For this reason trapezium shaped signals of steep slopes were assumed. A rise and decay time of these impulses are very small (3 s) comparing with the time constant ($\tau_g = 13502.86$ s). Introduced error has no significance and trapeziums will be treated in the following considerations as rectangulars.

Determination of the transient temperature field requires three stages of computations, always starting at the moment $t = 0$. In the consecutive steps the source was defined as follows:

$$g(x,y,z,t) = g(x,y,z)\begin{cases} \mathbf{1}(t) & \text{for } 0 \leqslant t \leqslant t_1, \\ [\mathbf{1}(t) - \mathbf{1}(t-t_1)] & \text{for } 0 \leqslant t \leqslant t_1 + t_2, \\ [\mathbf{1}(t) - \mathbf{1}(t-t_1) & \\ \quad + \mathbf{1}(t-t_1-t_2)] & \text{for } 0 \leqslant t \leqslant t_1 + t_2 + t_3, \end{cases} \tag{26}$$

and the system thermal response $T(x,y,z,t)$ was determined numerically in the adequate time interval. At the same time the moments t_1, t_2, t_3 were determined from the conditions (13), (18), (23) adequately reducing the time step in the surroundings of T_H or T_L. This way the program automatically changed the non-homogeneous equation of a diffusion (24), (25) onto homogeneous (and vice versa) at the moments of the cable power supply changes. Afterwards the program determined the initial conditions for the next stage of computations.

The computation of $T(x,y,z,t)$ for $0 \leqslant t \leqslant t_1 + t_2 + t_3$ terminates the procedure within the range of a full cycle of the power supply.

3.3. Criterion of averaging time constant

Relations (12), (17) and (22) are rather complex. They contain infinite number of components, in which each of them vanishes with different time constants τ_{mni}. The mentioned formulas can be substituted by more simple expressions. For that purpose the criterion of averaging time constant is applied (Section 2.2). According to that, it should be substituted in (12), (17), (22)

$$\tau_{mni} \to \tau(x,y,z), \tag{27a}$$

where $\tau(x,y,z)$ was determined by (8a) and (8b). In the consequence of the substitution of (27a), the expression in cubic brackets (concern (22)) or in square brackets (concern (17) and (7a)) will move before the symbol of a quadruple sum. A subsequent simplification was obtained after the substitution

$$\tau(x,y,z) \to \tau_{\mathrm{g}}, \tag{27b}$$

where τ_{g} is determined by (8c). In the discussed method the moments of the power supply switch-over are also determined from (13), (18) and (23).

Substitutions (27a) and (27b) change the system distributed parameters on concentrated ones at a given point of space. This is a reason for the errors introduced by the method discussed.

3.4. Superposition of step characteristics (heat-up curves)

Applying one of the above direct methods (Sections 3.1–3.3) the moment of first (t_1) and second $(t_1 + t_2 + t_3)$ switching off and repeated switching on $(t_1 + t_2)$ can be computed on the basis of (13), (18) and (23). The required solution follows from the system linearity [1,2] and the bottom line of formula (26):

$$\begin{aligned} T(x,y,z,t) = {} & H(x,y,z,t)\mathbf{1}(t) - H(x,y,z,t-t_1)\mathbf{1}(t-t_1) \\ & + H(x,y,z,t-t_1-t_2)\mathbf{1}(t-t_1-t_2) \\ & \text{for } 0 \leqslant t \leqslant t_1 + t_2 + t_3. \end{aligned} \tag{28}$$

Formula (28) is a superposition of the heater step characteristics (Section 2). After prior determination of t_1, t_2, t_3, relation (28) is very useful for the analysis of the system operation.

3.5. Examples of computations of the working cycle and discussion of the results

The relations and procedures presented in Sections 3.1–3.4 allow us to determine the time-spatial distribution of the system temperature. Computations were performed for a repeatable segment (Fig. 2). For the simulation a set of data was assumed from Section 2.4, which was supplemented as follows: $T_L = 25.5$°C, $T_H = 26.5$°C, $x^* = 0.9$ m, $y^* = 0.06$ m, $z^* = 0.5$ m. Therefore a location of the sensor of the regulator was chosen on the beginning of a "warm zone" of the heater surface [2, Fig. 5, where considering symmetry the co-ordinate $z^* = 0.5$ m refers to $z = 2.0$ m]. In consequence of that, the temperature of the warmest points will be close to the set temperature. Successively, $x^* = 0.09$ m ensures the same distance of the sensor from the warmest and coldest cross-sections of the investigated segment. Hence the sensor will be placed in the middle between the cable $x = x_1 = 0.06$ m and the maximal distance from it $x = 2a^* = 0.12$ m. Similar like in Section 2.4 the computations were realised by means of the computer Pentium II 233 MHz.

A convergence of the series (12), (17) and (22) was controlled in a manner described at the end of Section 2.1. The location of the point of the worst convergence and the number of considered terms of the series (12) were given in Section 2.4. In order to achieve a required convergence in (17) and in the transient component from formula (22), $325 \times 1564 \times 4756$ and $333 \times 1564 \times 4756$ terms were summated, respectively, at the initial moment of the proper time interval (i.e. at $t = t_1$ for (17) and at $t = t_1 + t_2$ for (22)). In both cases the number of considered terms rapidly declined with the time increase (up to $11 \times 11 \times 11$).

The results of direct computations (Sections 3.1–3.3) are presented in Fig. 6. The analytical and numerical methods enabled precise determination of the moments of the system switch-over. From the analytical method it was obtained that $t_1 = 11120$ s, $t_2 = 2911$ s, $t_3 = 4081$ s and the time of the cycle persistence $t_2 + t_3 = 6992$ s (therefore the interval of the power supply switching off

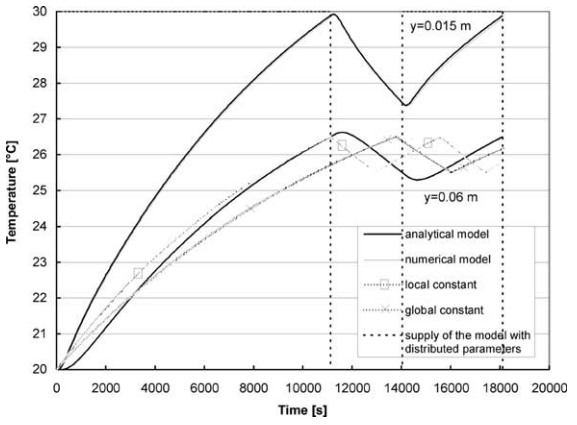

Fig. 6. Time-profiles of temperature for $x = 0.09$ m, $z = 0.5$ m.

occupies about 41.63% of the whole cycle). From the method of finite elements it follows that $t_1 = 11120$ s, $t_2 = 2935$ s, $t_3 = 4105$ s, $t_2 + t_3 = 7040$ s (and respectively about 41.69%). Because the global time constant is $\tau_g = 13502.86$ s (Fig. 3) the noticed differences have no significance.

The shape of the curves in Fig. 6 shows also the effects of a thermal inertia. Despite the power switch-over the system preserves a direction of the temperature changes at the moments t_1 and $t_1 + t_2$. However the system inertia is larger at the consecutive switching on $(t = t_1 + t_2)$ than during switching off $(t = t_1)$; because it is more difficult to force consecutive heating of concrete, than to allow for its free cooling off.

The estimation of usefulness of the averaging time constant during the start-up (for $0 \leqslant t \leqslant t_1$) was given in Section 2.4. As it is seen in Fig. 6, the accuracy of this method is considerably lower at the interval $t_1 \leqslant t \leqslant t_1 + t_2 + t_3$. It results from summation of the errors of an approximation during the system switch-over; because each point of the heater is substituted by a concentrated element of the first order, which does not model the inertia processes. In the consequence of the above, the results obtained by the method of averaging time constant are not presented in the next examples. However it is useful for a determination of the percentage share of the switching off period in the total cycle (ca. 40.89%). Hence, the method enables a correct estimation of the costs of the electrical energy consumption.

The intervals in which the successive switching off (t_2') and on (t_3') of the system take place follow from the conditions (29a), (29b):

$$T(x^*, y^*, z^*, t_1 + t_2 + t_3 + t_2') = T_L, \tag{29a}$$

$$T(x^*, y^*, z^*, t_1 + t_2 + t_3 + t_2' + t_3') = T_H. \tag{29b}$$

On this basis it was determined by means of the numerical method (Section 3.2) that $t_2' = t_2 - 22s$, $t_3' = t_3 + 11s$, where $t_2 = 2935$ s, $t_3 = 4105$ s. Because quantities of two orders less usually are neglected it was assumed that $t_2' = t_2$, $t_3' = t_3$. Such a simplification can be additionally justified as follows:

(a) A partial compensation of the differences with different signs (−22 s, +11 s) occurs within the supply cycle $t_2 + t_3 = 7040$ s.
(b) The value of the differences is very small comparing with the system global time constant $\tau_g = 13503$ s (Fig. 3).

In these conditions the solution $T(x, y, z, t)$ for $0 \leqslant t \leqslant t_1 + 2t_2 + 2t_3$ was obtained adding the relation

$$-H(x, y, z, t - t_1 - t_2 - t_3)\mathbf{1}(t - t_1 - t_2 - t_3) + H(x, y, z, t - t_1 - 2t_2 - t_3)\mathbf{1}(t - t_1 - 2t_2 - t_3), \tag{30}$$

to the right-hand side of (28). On this basis Figs. 7(a)–(c) were prepared. As it is seen, within the investigated time interval (about 7 h) three types of temperature profiles appeared. The differences between them follow from a dependence of the heat diffusion velocity on a distance from the cable; because the inertia effects are diminished approaching the heat source.

At the region most distant from the cable (for $z \in \langle 0, 0.2ul\rangle \cup \langle (1 - 0.2u)l, l\rangle$) the temperature is slowly (but permanently) increasing (Fig. 7(a)). The thermal inertia of this zone is so large that for $0 \leqslant t \leqslant t_1 + 2t_2 + 2t_3$ a lack of reaction occurs on switching off of the system power supply (at the moment $t = t_1$ and $t = t_1 + t_2 + t_3$). There are the following reasons for such a situation:

(a) At the boundary region the apparent dead time (ca. 4000 s, Fig. 7(a)) is larger than the time of the energy switching off $(t_2 = 2935$ s).
(b) Time constant of the points of the considered peripheral area (over 27 000 s, Fig. 3) is considerably larger than the supply break t_2.

For $z \in \langle 0.3ul, 0.9ul\rangle \cup \langle (1 - 0.9u)l, (1 - 0.3u)l\rangle$ the temperature profiles are aperiodic increasing and declining (Fig. 7(b)). As it is seen, the ranges of the temperature rise and decline do not overlap the intervals of the system switching on and off (for $t_1 \leqslant t \leqslant t_1 + 2t_2 + 2t_3$). A slow heat diffusion in that region is responsible for a delay of the heater reaction.

In the region of the resistive cable (for $z \in \langle ul, (1 - u)l\rangle$) the temperature profiles are oscillatory for $t \geqslant t_1$ (Figs. 6 and 7(c)). The temperature difference at the same points of the area discussed but at the moments differed of $t_2 + t_3$ was investigated. It occurred that the largest deviation of a cyclic value appears on the cable surface and does not exceed 0.07°C. This insignificant aberration allows us to consider the temperature profiles as quasi-cyclic within the given range of variables (z, t). The difference between the maximum and minimum of the repeatable cycle can be a measure of the thermal oscillations. The largest oscillations proceed in the plane

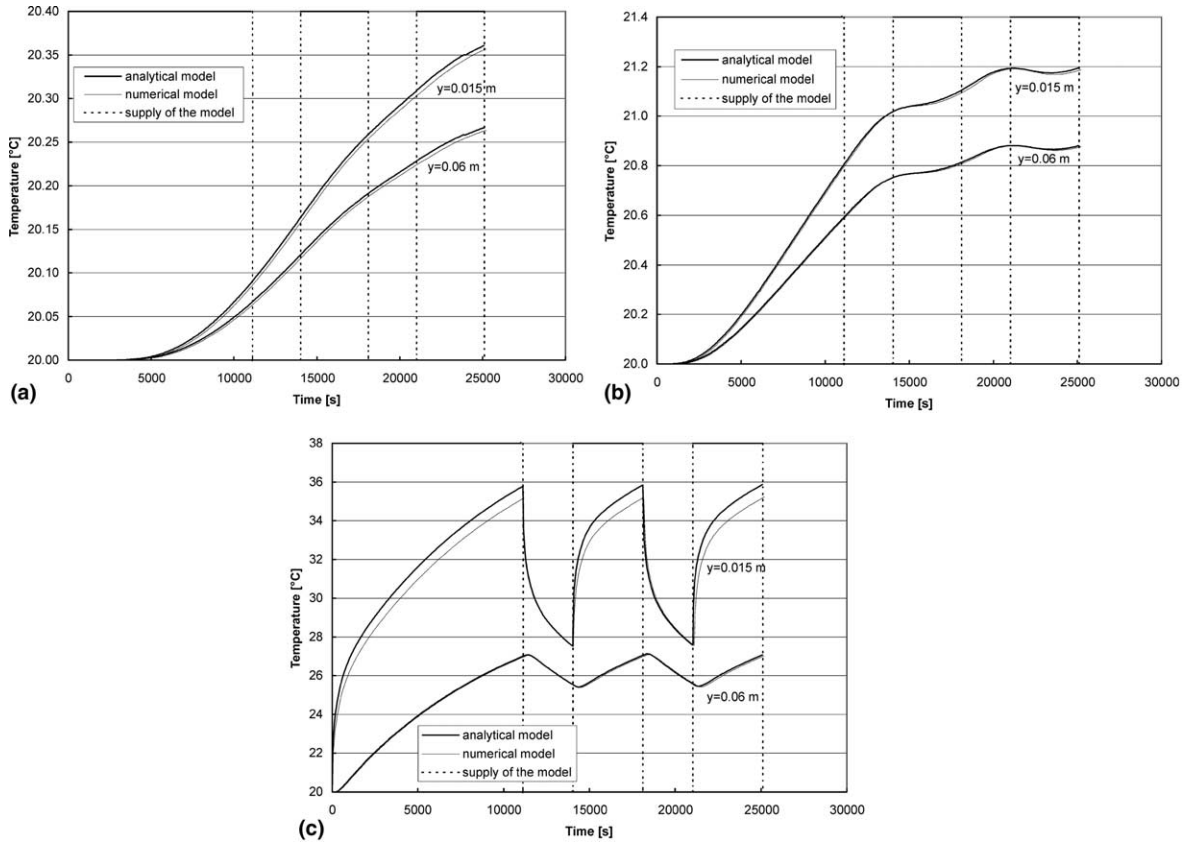

Fig. 7. Time-profiles of temperature for $x = 0.06$ m: (a) $z = 0.05$ m; (b) $z = 0.15$ m; (c) $z = 1.25$ m.

of the cable ($y = y_1 = 0.015$ m), but they are considerably smaller on the surface of the heater ($y = 2b = 0.06$ m, Figs. 6 and 7(c)). The dumping effect of the floor plate follows not only from the difference of the heat diffusion velocity on the specified planes of the panel. The heat accumulation in the concrete layer of the thickness $2b - y_1 = 0.045$ m also introduces its influence.

In formulas (28) and (30) the step characteristics of the system determined analytically or numerically (Sections 2.1 and 2.3) are present. The largest difference between the analytical and numerical solution is located in the nearest surroundings of the cable (Fig. 7(c), $y = y_l = 0.015$ m). It follows from different models of the cable core assumed in the respective models (Section 2.4, point (c)]. When the cable is not energised and the region becomes source-free (i.e. for $t \in \langle t_1, t_1 + t_2\rangle \cup \langle t_1 + t_2 + t_3, t_1 + 2t_2 + t_3\rangle$) the discussed difference vanishes.

The consecutive step profiles appropriately shifted in time can be added to (28), (30). This way the time-spatial temperature distributions for $t > t_1 + 2t_2 + 2t_3$ are determined. With the time increase the following changes proceed:

(a) monotonically increasing profiles transform into aperiodic decreases and increase of the temperature,
(b) aperiodic profiles become oscillatory.

After obtaining the steady state ($t \to \infty$), the temperature is cyclically varied in time in the whole volume of the heater.

4. Conclusion

The analysis of a regime of an electric direct heating floor has been presented in the paper. It was proved that the thermal field in the device strongly changes in time and space. For this reason determination of:

(a) time constant (Fig. 3),
(b) heating on curve (Figs. 4 and 5),
(c) starting and working cycle of the system (Figs. 6 and 7)

has important practical meaning. The specified parameters and characteristics were computed by different methods and discussed in detail in Sections 2.4 and 3.5. This way a three-dimensional image of dynamics of the modelled heater has been obtained.

Acknowledgements

The paper was prepared in Technical University of Białystok within a framework of the project W/WE/2/99 financed by the State Committee for Scientific Research, Poland.

References

[1] J. Gołębiowski, W. Peterson, Stationary thermal field in a long duct of an electrical heating system, Electr. Eng. – Archiv für Elektrotechnik 79 (1) (1996) 17–22.
[2] J. Gołębiowski, S. Kwiecèkowski, Analytical and numerical modelling of a stationary temperature field in a three dimensional electric heating system, Electr. Eng. – Archiv für Elektrotechnik 81 (2) (1998) 69–76.
[3] S. Kwiećkowski, J. Gołębiowski, Transient thermal field in a long duct of an electrical floor heating. Part I. Step response of the system. Part II. Operation with a regulator, Arch. Electr. Eng. XLVIII (4) (1999) 429–452.
[4] Y. Takahashi, M.J. Rabins, D.M. Auslander, Control and Dynamic Systems, Addison-Wesley, Reading, MA, 1972.
[5] W. Lipiński, E. Kornatowski, Über die Eindringzeit des elektromagnetisches Feldes in einer zylindersymmetrischen Abschirmung, Arch. Electr. Eng. XLIII (3) (1994) 663–667.
[6] J. Gołębiowski, W. Lipiński, Modelling of electromagnetic shield dynamics, IEEE Trans. Magn. 16 (6) (1980) 1419–1422.
[7] D. Hofmann, Dynamische Temperaturmessung, Verlag Technik, Berlin, 1976.
[8] G. Lehner, Elektromagnetische Feldtheorie, Springer, Berlin, 1996.
[9] J.P. Holman, Heat Transfer, McGraw-Hill, New York, 1986.
[10] K.J. Bathe, Finite-Elemente Methoden, Springer, Berlin, 1990.
[11] O.C. Zienkiewicz, The Finite Element Method, McGraw-Hill, London, 1989.
[12] User's Manual for NISA II, Numerically Integrated Elements for Systems Analysis, Engineering Mechanics Research Corporation (EMRC), Troy-Michigan, 1991.
[13] G. Feirweather, Finite Element Galerkin Methods for Differential Equations, Marcel Dekker, New York, 1978.
[14] J.V. Beck, K.D. Cole, A. Haji-Sheikh, B. Litkouhi, Heat Conduction Using Green's Functions, Hemisphere, London, 1992.
[15] W. Baade, Elektrische Raumheiztechnik. Installieren, Warten, Prüfen, Verlag Technik, Berlin, 1995.
[16] M. Palic, Elektrische Wärme-und Heiztechnick, Expert Verlag, Ehningen bei Böblingen, 1992.
[17] K.T. Januszkiewicz, Numerical model of the periodical operation of the electric storage floor heating, Arch. Electr. Eng. XLIV (3) (1995) 427–437.
[18] S.C. Tendon, A.F. Armor, M.K.K. Chari, Nonlinear transient finite element field computation for electrical machines and devices, IEEE Trans. PAS-102 (5) (1983) 1089–1096.